Sufficient Statistics, Classification, and a Novel Approach for Frame Detection in OFDM Systems

Hamed Abdzadeh-Ziabari and Mahrokh G. Shayesteh, *Member, IEEE*

***Abstract*—This paper addresses the problem of frame detection in orthogonal frequency-division multiplexing (OFDM) systems. Using fourth-order statistics, a novel approach is presented for detection of a preamble composed of two identical parts in the time domain. First, it is demonstrated that sufficient statistics for detection of a periodic preamble do not exist, and conventional methods are not optimal. Next, looking at the detection of a preamble from the viewpoints of hypothesis testing and classification, a new method is presented based on the idea that fourth-order statistics can increase class separability (between-class distance) and consequently improve detection performance. It is proven that the proposed method has a considerably lower probability of false alarm. Along with the missed-detection performance comparisons, it will be presented that the new scheme offers a superior detection performance and makes threshold selection significantly easier.**

***Index Terms*—Classification, detection, orthognal frequency-division multiplexing (OFDM), preamble, synchronization.**

I. Introduction

ORTHOGONAL frequency-division multiplexing (OFDM), which has been utilized in many wireless systems such as digital video broadcasting, wireless metropolitan area networks, and wireless local area networks, is sensitive to carrier frequency and timing offsets. To make the OFDM-based systems have acceptable performance, these offsets should be estimated and compensated for.

Methods that deal with timing estimation in OFDM systems fall into two categories: blind methods [1], [2], and those that use one or more preambles at the start of the frame [3]–[14]. Methods of the second category, which is the focus of this paper, usually utilize a preamble with two or more identical parts in the time domain. These schemes estimate the start of the frame in a two-step procedure. The first step is frame detection that is achieved when a timing metric reaches a predefined threshold, and the second step is a coarse estimation of the start of the frame using the maximum of a timing metric. Schmidl and Cox [3] used the autocorrelation between the two identical parts of a preamble for timing synchronization. In [4] and [5], Minn *et al.* used a preamble with more than two identical parts in the time domain and changed the signs of some of the identical parts to have a sharper timing metric. Colusion [6] presented an algorithm for timing estimation similar to [3] and analyzed its performance in [7]. In [8], Shi and Serpedin proposed a timing estimator based on the maximum-likelihood (ML) approach that takes advantage of a preamble with a structure similar to [5]. For having a lower probability of false alarm, Ruan *et al.* [9] presented a method that can use the periodic parts of more than one preamble, and their method is reduced to a metric equivalent to [3] when used for a preamble with two identical parts. There are methods [10]–[12] that produce an impulse-like timing metric using the cross correlation of the received signal with the known preamble. In fading channels, these methods do not have the robustness of the autocorrelation metrics and are affected by channel distortion. Furthermore, the receiver needs to know exactly the preamble signal that can be complex when the preamble is selected from a large number of candidates to identify the cell or sector index [13]. There are also methods [13], [14] that jointly estimate the start of the frame and carrier frequency offset (CFO) using the ML principle.

In this paper, we look at frame detection from the viewpoints of hypothesis testing and classification. We first demonstrate that sufficient statistics for frame detection do not exist, and consequently, conventional methods are not optimal.

We consider the design of a timing metric as a feature selection problem. Knowing that the feature selection procedure is to choose those components that are most effective for separating different classes [15], we introduce the utilization of fourth-order statistics in the timing metric for frame detection. The use of fourth-order statistics is proven beneficial for an unknown signal detection and classification [16], [17]. Here, we use the fourth-order statistics for detection of a sequence of known signals (the preamble is known to have two identical parts) in OFDM systems. Using the means of the timing metrics and also the well-known Fisher's discriminant ratio (FDR) as the criteria for class separability [15], [18], we show that the new timing metric is a better detector (classifier) since it can significantly increase the distance and distinctions between the two classes (presence and absence of the preamble), in comparison with the previous metrics.

Considering the fact that the main factor affecting the false alarm probability is the correlation length, (the longer the correlation length, the lower the false alarm probability), we point out that, because of having an increased correlation length, the new timing metric has a remarkably lower probability of false alarm. It will be finally demonstrated that when the new detection scheme is used in coarse timing estimation, not only

Manuscript received August 20, 2012; revised October 26, 2012 and December 2, 2012; accepted January 5, 2013. Date of publication January 14, 2013; date of current version July 10, 2013. The review of this paper was coordinated by Dr. T. Jiang.

H. Abdzadeh-Ziabari is with the Department of Electrical Engineering, Urmia University, Urmia, Iran (e-mail: st_h.abdzadeh@urmia.ac.ir).

M. G. Shayesteh is with the Department of Electrical Engineering, Urmia University, Urmia, Iran. She is also working with the Wireless Research Laboratory, Advanced Communications Research Institute, Sharif University of Technology, Tehran, Iran (e-mail: m.shayesteh@urmia.ac.ir).

Color versions of one or more of the figures in this paper are available online at http://ieeexplore.ieee.org.

Digital Object Identifier 10.1109/TVT.2013.2240027

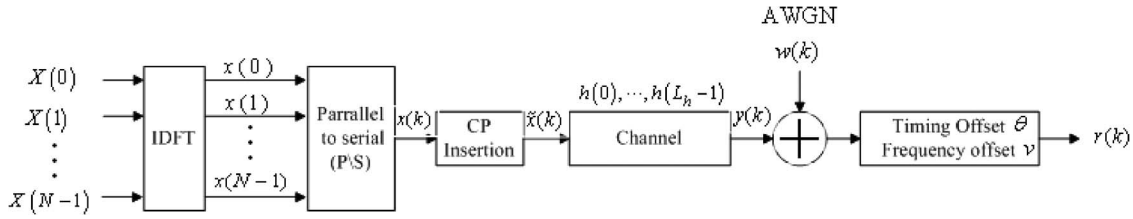

Fig. 1. The block diagram of an OFDM system with N subcarriers.

can it significantly extend the range of threshold values for which an acceptable performance exists, but its combination with previous detectors can also provide a remarkably wider range of suitable thresholds and make the critical task of threshold selection for detection of the frame considerably easier.

The rest of this paper is organized as follows. In Section II, the OFDM system is described. Section III investigates the sufficiency of the statistics used in the conventional methods. Section IV is dedicated to the proposed method, and Section V presents the analytical performance evaluation of the new method. In Section VI, we address the computational complexity and frame synchronization. Simulation results are provided in Section VII. Finally, Section VIII presents the conclusion.

II. System Description

Considering an OFDM system with N subcarriers, the samples of an OFDM symbol in the time domain given by

$$x(k) = \frac{1}{\sqrt{N}} \sum_{n=0}^{N-1} X(n) e^{j2\pi k \frac{n}{N}}, \quad 0 \le k \le N-1 \qquad (1)$$

are generated by utilizing the N-point inverse fast Fourier transform (IFFT) on the information symbols $X(n)$, $0 \le n \le N-1$. For mitigation of intersymbol interference (ISI), a cyclic prefix (CP) of length G is appended in front of $x(k)$ as follows:

$$\tilde{x}(k) = \begin{cases} x(k+N), & -G \le k \le -1 \\ x(k), & 0 \le k \le N-1. \end{cases} \qquad (2)$$

The length of the CP is longer than the length of the channel impulse response (CIR). After transmission over a frequency-selective fading channel, the received signal is expressed as

$$r(k) = e^{j\frac{2\pi}{N}k\,v} y(k-\theta) + w(k), \quad -G \le k \le N + L_h - 2 \qquad (3)$$

where

$$y(k) = \sum_{l=0}^{L_h-1} h(l)\, \tilde{x}(k-l). \qquad (4)$$

Furthermore, in (3), θ is the timing offset, v is the CFO normalized by the subcarrier spacing $1/T$ (T is an OFDM symbol interval), and $w(k)$ is a sample of additive white Gaussian noise with zero mean and variance σ_w^2. $h(l)$, $l = 0, 1, \ldots, L_h - 1$, is the CIR of the frequency-selective fading channel, and L_h is the length of the CIR. In Fig. 1, we have depicted the block diagram of the described OFDM system.

We assume packet-based OFDM systems in which OFDM frames are preceded by noise samples, and at least one preamble is placed at the start of the frame for the purpose of timing and frequency synchronization and channel estimation. The transmitter sends a preamble composed of two identical parts in the time domain. The preamble vector in the time domain is denoted by $\mathbf{s} = [s(0), s(1), \ldots, s(N-1)]^T$, where $s(k)$ is the kth element of $\mathbf{s}$, and C^T denotes the transpose of the vector C. Such a preamble can be generated by transmission of a pseudonoise sequence on the even subcarriers and a zero sequence on the odd subcarriers. A preamble with this structure is widely used in practical applications such as WiMAX systems [19]. Since by detection of the preamble, a frame is detected, we concentrate on the preamble detection.

III. Hypothesis Testing, Classification, and Sufficient Statistics for Frame Detection

Here, we briefly discuss frame detection from the viewpoints of hypothesis testing and classification and then address the important issue of sufficient statistics in frame detection.

A. Frame Detection as Hypothesis Testing and Classification

Correlation-based hypothesis testing has been used for detection of a frame in OFDM systems in [3] and [9]. In hypothesis testing for frame detection, we deal with a timing metric and two hypotheses: the null hypothesis H_0, which indicates the absence of the preamble, and the alternative hypothesis H_1, which represents the presence of the preamble. In other words, using a timing metric, we are interested in knowing which of the following hypotheses is correct:

H_0: absence of the preamble;

H_1: presence of the preamble.

When the value of a timing metric is greater than a predefined threshold λ, the presence of the preamble is announced, and when the timing metric falls below the predefined threshold, the absence of the preamble is declared.

The problem is choosing the timing metric that can efficiently detect the frame when the received vector at time instant d, i.e., $\mathbf{r}^d = [r(d), r(d+1), \ldots, r(d+N-1)]^T$ is observed. This problem, in classification theory, is referred to as the problem of feature selection for two classes (the absence or presence of a preamble). In other words, we want to know how the timing metric should be designed to enable us to choose the components from the received vector that are most effective for separating the two classes [15]. If features with little discrimination power are selected, the design of the classifier

(timing metric) would lead to poor performance. Hence, we should aim at selecting features that lead to large between-class distances [18].

With this goal in mind (i.e., looking for timing metrics with larger between-class distances), we first investigate the conventional timing metrics, and indicate that they are not optimal and do not use the sufficient statistics. We use this fact to draw the conclusion that it is possible to have better detectors than the conventional detectors.

B. Sufficient Statistics for Frame Detection and Optimality of the Conventional Methods

We consider a preamble $\mathbf{s}=[s(0), s(1), \ldots, s(N-1)]^T$ with two identical parts in the time domain i.e., $\mathbf{s}=[A, A]^T$, where $A=\{s(0), s(1), \ldots, s((N/2)-1)\}$ is a subvector of $\mathbf{s}$. To examine the optimality of the conventional methods, we investigate whether the conventional methods use sufficient statistics or not.

After observing the received vector $\mathbf{r}=[r(0), r(1), \ldots, r(N-1)]^T$, we generate the following vectors using the real and imaginary parts of the first and second halves of $\mathbf{r}$ as

$$\mathbf{r_1}=\{r_r(0), r_i(0), r_r(1), r_i(1), \ldots, r_r\left((N/2)-1\right), r_i\left((N/2)-1\right)\} \tag{5}$$

$$\mathbf{r_2}=\{r_r(N/2), r_i(N/2), r_r\left((N/2)+1\right), r_i\left((N/2)+1\right), \ldots, r_r(N-1), r_i(N-1)\} \tag{6}$$

where $r_r(k)$ and $r_i(k)$ are the real and imaginary parts of $r(k)$, respectively. Furthermore, $r_r(k)$ and $r_i(k)$ are zero-mean random variables that are independent and identically distributed. For the kth elements of $\mathbf{r_1}$ and $\mathbf{r_2}$, i.e., $r_1(k)$ and $r_2(k)$, we have the following two Gaussian probability distribution functions (pdfs) [20] for the two hypotheses:

$$f\left(r_1(k), r_2(k)|\, H_0\right) = \frac{1}{2\pi\sigma_0^2}\exp\left(-\frac{r_1^2(k)+r_2^2(k)}{2\sigma_0^2}\right) \tag{7}$$

$$f\left(r_1(k), r_2(k)|\, H_1\right) = \frac{1}{2\pi\sigma_1^2\sqrt{1-\rho_1^2}} \times \exp\left(-\frac{r_1^2(k)+r_2^2(k)-2\rho_1 r_1(k) r_2(k)}{2\left(1-\rho_1^2\right)\sigma_1^2}\right) \tag{8}$$

where $\sigma_0^2=\sigma_w^2/2$, $\sigma_1^2=(\sigma_y^2+\sigma_w^2)/2$, $\rho_1=(\sigma_y^2)/(\sigma_y^2+\sigma_w^2)=\mathrm{SNR}/(\mathrm{SNR}+1)$, and $\sigma_y^2=E\{|y(k)|^2\}$.

It is well known that the Neyman–Pearson optimization criterion (which aims at obtaining the best possible detection performance while guaranteeing that the false alarm probability does not exceed some tolerable value) results in the likelihood ratio test [21]. Hence, for the aforementioned pdfs, the Neyman–Pearson optimality criterion leads to the following likelihood ratio:

$$\begin{aligned}\Lambda(\mathbf{r_1}, \mathbf{r_2}) &= \frac{\prod_{k=0}^{N-1} f\left(r_1(k), r_2(k)|\, H_1\right)}{\prod_{k=0}^{N-1} f\left(r_1(k), r_2(k)|\, H_0\right)} \\ &= \frac{\prod_{k=0}^{N-1} \frac{1}{2\pi\sigma_1^2\sqrt{1-\rho_1^2}}\exp\left(-\frac{r_1^2(k)+r_2^2(k)-2\rho_1 r_1(k) r_2(k)}{2\left(1-\rho_1^2\right)\sigma_1^2}\right)}{\prod_{k=0}^{N-1} \frac{1}{2\pi\sigma_0^2}\exp\left(-\frac{r_1^2(k)+r_2^2(k)}{2\sigma_0^2}\right)}\end{aligned} \tag{9}$$

which reduces to

$$\begin{aligned}\Lambda(\mathbf{r_1}, \mathbf{r_2}) &= \frac{\sigma_0^{2N}}{\sigma_1^{2N}\left(\sqrt{1-\rho_1^2}\right)^N} \\ &\quad\times \exp\left(\left(\frac{1}{2\sigma_0^2}-\frac{1}{2\left(1-\rho_1^2\right)\sigma_1^2}\right)\sum_{k=0}^{N-1}\left(r_1^2(k)+r_2^2(k)\right) + \frac{\rho_1}{\left(1-\rho_1^2\right)\sigma_1^2}\sum_{k=0}^{N-1} r_1(k) r_2(k)\right).\end{aligned} \tag{10}$$

Since no more simplification is possible for $\Lambda(\mathbf{r_1}, \mathbf{r_2})$, sufficient statistics do not exist [22].

To give more explanation, we obtain the natural logarithm of $\Lambda(\mathbf{r_1}, \mathbf{r_2})$ and have

$$\begin{aligned}\Upsilon(\mathbf{r_1}, \mathbf{r_2}) &= \ln\left(\frac{\sigma_0^{2N}}{\sigma_1^{2N}\left(\sqrt{1-\rho_1^2}\right)^N}\right) \\ &\quad + \left(\frac{1}{2\sigma_0^2}-\frac{1}{2\left(1-\rho_1^2\right)\sigma_1^2}\right)\sum_{k=0}^{N-1}\left(r_1^2(k)+r_2^2(k)\right) \\ &\quad + \frac{\rho_1}{\left(1-\rho_1^2\right)\sigma_1^2}\sum_{k=0}^{N-1} r_1(k) r_2(k).\end{aligned} \tag{11}$$

Next, we compare $\Upsilon(\mathbf{r_1}, \mathbf{r_2})$ with a threshold λ. Therefore, we have

$$\begin{aligned}&\left(\frac{1}{2\sigma_0^2}-\frac{1}{2\left(1-\rho_1^2\right)\sigma_1^2}\right)\sum_{k=0}^{N-1}\left(r_1^2(k)+r_2^2(k)\right) \\ &\quad + \frac{\rho_1}{\left(1-\rho_1^2\right)\sigma_1^2}\sum_{k=0}^{N-1} r_1(k) r_2(k) \\ &\quad > \lambda - \ln\left(\frac{\sigma_0^{2N}}{\sigma_1^{2N}\left(\sqrt{1-\rho_1^2}\right)^N}\right).\end{aligned} \tag{12}$$

It is observed that we cannot arrange (12), so that the left-hand side of (12) only includes those terms explicitly containing $r_1(k)$ and $r_2(k)$, and all other constants are moved to the right-hand side of (12). Hence, neither the sufficient statistics exist [21] nor does the conventional methods use the sufficient statistics. Note that if the sufficient statistics exist for an arbitrary hypothesis

$$\begin{aligned} H_0 &: \theta = \theta_0 \\ H_1 &: \theta = \theta_1 \end{aligned} \tag{13}$$

then according to the Neyman–Fisher factorization theorem, we can express the pdfs as $f(x;\theta_0) = g(T(x),\theta_0)h(x)$ and $f(x;\theta_1) = g(T(x),\theta_1)h(x)$. (Note that, notations $f(x;\theta_0)$ and $f(x;\theta_1)$ represent families of pdfs and should not be confused with the joint pdfs.) Consequently, the likelihood ratio becomes [22] $(f(x;\theta_1)/f(x;\theta_0)) = g(T(x),\theta_1)/g(T(x),\theta_0)$, which means that, if the sufficient statistics exist, the likelihood ratio or, equivalently, the log-likelihood ratio depends on x only through $T(x)$, where $T(x)$ is only a function of x, and not any other parameters or constants. Therefore, for $\Upsilon(\mathbf{r_1},\mathbf{r_2})$ in (11), since we cannot find any functions that are only dependent on $r_1(k)$ and $r_2(k)$ and not any other parameters or constants, the sufficient statistics do not exist. This statement is tantamount to saying that, since (12) cannot be arranged in the way that the left-hand side of (12) only includes those terms explicitly containing $r_1(k)$ and $r_2(k)$ (without any constants or other parameters), and the right-hand side of (12) contains all other constants, the sufficient statistics do not exist [21].

In conclusion, having the pdfs in (7) and (8), an optimal detector that uses the sufficient statistics does not exist. This important conclusion is the motivation for the presentation of a new method with better performance than the conventional methods as follows.

IV. Proposed Method

For detection of a preamble with two identical parts $\mathbf{s} = [A, A]^T$, where $A = \{s(0), s(1), \ldots, s((N/2)-1)\}$ is a subvector of $\mathbf{s}$, the conventional methods take advantage of the repetitive structure of the preamble, and use the addition of the following second-order elements for correlation:

$$\begin{aligned} &\overline{r}(d)r\left(d+(N/2)\right),\ \overline{r}(d+1)r\left(d+(N/2)+1\right),\ldots, \\ &\qquad \overline{r}\left(d+(N/2)-1\right)r(d+N-1) \end{aligned} \tag{14}$$

where $\overline{r}(d)$ denotes the complex conjugate of $r(d)$. When the preamble $\mathbf{s} = [A, A]^T$ is present, $y(k)$ in (4) remains periodic (A preamble composed of two identical parts in the time domain remains periodic in a frequency-selective fading channel as long as the length of the channel delay spread is smaller than the length of each identical part of the preamble.) The received vector $\mathbf{r}^d = [r(d), r(d+1), \ldots, r(d+N-1)]^T$ when the preamble is present (at the time instant $d = \theta$) can be written as $\mathbf{r}^\theta = [r(\theta), r(\theta+1), \ldots, r(\theta+N-1)]^T$. Considering (3), we have

$$\begin{aligned} \mathbf{r}^\theta = \Big[&e^{j\frac{2\pi}{N}\theta v}y(0) + w(\theta),\ e^{j\frac{2\pi}{N}(\theta+1)v}y(1) + w(\theta+1),\ldots, \\ &e^{j\frac{2\pi}{N}(N-1+\theta)v}y(N-1) + w(N-1+\theta)\Big]^T. \end{aligned} \tag{15}$$

Assuming for simplification that noise is negligible, (without any effect on the following analysis and since we want to concentrate on the value of the correlation function of conventional timing metrics resulting from the preamble part of the received signal), i.e.,

$$\mathbf{r}^\theta = \left[e^{j\frac{2\pi}{N}\theta v}y(0), e^{j\frac{2\pi}{N}(\theta+1)v}y(1),\ \ldots,\ e^{j\frac{2\pi}{N}(N-1+\theta)v}y(N-1)\right]^T \tag{16}$$

and taking into account the fact that

$$y(k) = y\left(k+(N/2)\right), \quad k = 0, 1, \ldots, (N/2)-1 \tag{17}$$

then (14) becomes

$$\begin{aligned} &e^{j\frac{2\pi}{N}v(N/2)}\overline{y}(0)y(0),\ e^{j\frac{2\pi}{N}v(N/2)}\overline{y}(1)y(1),\ldots, \\ &\qquad e^{j\frac{2\pi}{N}v(N/2)}\overline{y}\left((N/2)-1\right)\ y\left((N/2)-1\right). \end{aligned} \tag{18}$$

The absolute value of the summation of the elements of (18), which is the correlation function of conventional methods, produces the following peak when the preamble is present:

$$\begin{aligned} |P_R(d)| &= \left|\sum_{k=0}^{(N/2)-1}\overline{r}(d+k)r\left(d+k+(N/2)\right)\right| \\ &= \sum_{k=0}^{(N/2)-1}|y(k)|^2. \end{aligned} \tag{19}$$

Fourth-order statistics have been used for detection of an unknown signal in [16] and [17]. Here, we propose to use fourth-order statistics for preamble detection in OFDM systems. Now, instead of the second-order elements (14), we propose to utilize the following fourth-order elements

$$\begin{aligned} &\overline{r}(d)\overline{r}(d+1)r\left(d+(N/2)\right)r\left(d+(N/2)+1\right), \\ &\quad \overline{r}(d)\overline{r}(d+2)r\left(d+(N/2)\right)r\left(d+(N/2)+2\right), \\ &\quad \ldots, \overline{r}(d)\overline{r}\left(d+(N/2)-1\right)r\left(d+(N/2)\right)r(d+N-1), \\ &\overline{r}(d+1)\overline{r}(d+2)r\left(d+(N/2)+1\right)r\left(d+(N/2)+2\right), \\ &\quad \overline{r}(d+1)\overline{r}(d+3)r\left(d+(N/2)+1\right) \\ &\quad \times r\left(d+(N/2)+3\right), \ldots, \overline{r}(d+1)\overline{r}\left(d+(N/2)-1\right) \\ &\quad \times r\left(d+(N/2)+1\right)r(d+N-1), \\ &\quad \ldots, \overline{r}\left(d+(N/2)-2\right)\overline{r}\left(d+(N/2)-1\right) \\ &\quad \times r(d+N-2)r(d+N-1). \end{aligned} \tag{20}$$

In other words, instead of directly correlating the first half of the received vector $r(d),\ r(d+1), \ldots, r(d+(N/2)-1)$ with the second half of the received vector $r(d+(N/2)), r(d+(N/2)+1), \ldots, r(d+N-1)$, we generate the following sequence $B^{r1,d}$ from the first half of the received vector:

$$\begin{aligned} B^{r1,d} = \{&r(d)r(d+1), r(d)r(d+2), \\ &\ldots, r(d)r\left(d+(N/2)-1\right), \\ &r(d+1)r(d+2), r(d+1)r(d+3), \ldots, \\ &r(d+1)r\left(d+(N/2)-1\right), \\ &\ldots, r\left(d+(N/2)-2\right)r\left(d+(N/2)-1\right)\} \end{aligned} \tag{21}$$

and correlate it with the following corresponding sequence $B^{r2,d}$ from the second half of the received vector:

$$\begin{aligned} B^{r2,d} = \{&r\left(d+(N/2)\right) r\left(d+(N/2)+1\right), \\ &r\left(d+(N/2)\right) r\left(d+(N/2)+2\right), \\ &\ldots, r\left(d+(N/2)\right) r(d+N-1), \\ &r\left(d+(N/2)+1\right) r\left(d+(N/2)+2\right), \\ &r\left(d+(N/2)+1\right) r\left(d+(N/2)+3\right), \\ &\ldots, r\left(d+(N/2)+1\right) r(d+N-1), \\ &\ldots, r(d+N-2) r(d+N-1)\}. \end{aligned} \tag{22}$$

Therefore, the proposed correlation function can be expressed as

$$\begin{aligned} P_P(d) = &\sum_{k=0}^{(N/2)-2} \sum_{l=k+1}^{(N/2)-1} \overline{r}(d+k)\overline{r}(d+l) \\ &\times r\left(d+k+(N/2)\right) r\left(d+l+(N/2)\right). \end{aligned} \tag{23}$$

It is obvious that the number of the fourth-order elements $(N/4)((N/2)-1)$ in (20) is far greater than the number of second-order elements $(N/2)$ in (14). As demonstrated later, this significant increase in the number of the elements results in better class separability and detection performance.

It is observed that the absolute value of the correlation functions [$|P_R(d)|$ in (19) or $|P_P(d)|$ in the proposed method (23)] fluctuates with the received signal strength. For example, we know from Appendix B that, in the presence of the preamble, $E\{|P_P(\theta)|\} = L\sigma_y^4$, where L is the correlation length and $\sigma_y^2 = E\{|y(k)|^2\}$. To avoid the undesirable effects of the power fluctuations, the correlation function is normalized so that at the correct timing point, it produces values that have expectation approximately equal to 1 [9]. To do so, we consider the powers of the sequences $B^{r1,d}$ and $B^{r2,d}$. The power of these sequences at the correct timing point is obtained in Appendix B and given as

$$\begin{aligned} &E\left\{\sum_{k=0}^{(N/2)-2} \sum_{l=k+1}^{(N/2)-1} |r(d+k)r(d+l)|^2\right\} \\ &\quad = E\left\{\sum_{k=0}^{(N/2)-2} \sum_{l=k+1}^{(N/2)-1} \right. \\ &\qquad \left. |r\left(d+k+(N/2)\right) r\left(d+l+(N/2)\right)|^2\right\} \\ &\quad = L\left(\sigma_y^4 + 2\sigma_y^2\sigma_w^2 + \sigma_w^4\right). \end{aligned} \tag{24}$$

Hence, by defining

$$\begin{aligned} R_P(d) = &\sum_{k=0}^{(N/2)-2} \sum_{l=k+1}^{(N/2)-1} |r(d+k)r(d+l)|^2 \\ &+ \sum_{k=0}^{(N/2)-2} \sum_{l=k+1}^{(N/2)-1} |r\left(d+k+(N/2)\right) r\left(d+l+(N/2)\right)|^2 \end{aligned} \tag{25}$$

and knowing that $E\{R_P(\theta)\} = 2L(\sigma_y^4 + 2\sigma_y^2\sigma_w^2 + \sigma_w^4)$, the fluctuations of the signal power in the correlation function can be avoided by using

$$\begin{aligned} \frac{|P_P(\theta)|}{R_P(\theta)} &\approx \frac{E\left\{|P_P(\theta)|\right\}}{E\left\{R_P(\theta)\right\}} = \frac{L\sigma_y^4}{2L\left(\sigma_y^4 + 2\sigma_y^2\sigma_w^2 + \sigma_w^4\right)} \\ &= \frac{1}{2}\left(\frac{1}{1+(2/\text{SNR})+(1/\text{SNR})^2}\right). \end{aligned} \tag{26}$$

For high SNRs, we have $(|P_P(\theta)|/R_P(\theta)) \approx 1/2$.

Finally, the proposed timing metric is obtained by multiplication of $(|P_P(d)|/R_P(d))$ by the factor 2, so that the timing metric has values between 0 and 1. Consequently, the proposed timing metric is as follows:

$$M_P(d) = 2\frac{|P_P(d)|}{R_P(d)}. \tag{27}$$

When the preamble is present, ignoring the noise terms (as mentioned previously, without having any impact on the analysis, we neglect the noise term for simplification and concentration on the value of the correlation function of the new timing metric resulting from the preamble part of the received signal) and considering again (15)–(17), we have

$$\begin{aligned} P_P(d) = &\sum_{k=0}^{(N/2)-2} \sum_{l=k+1}^{(N/2)-1} e^{j\frac{2\pi}{N}(N/2)v} \overline{y}(k) y\left(k+(N/2)\right) \\ &\times e^{j\frac{2\pi}{N}(N/2)v} \overline{y}(l) y\left(l+(N/2)\right) \\ = &\, e^{j2\pi v} \sum_{k=0}^{(N/2)-2} \sum_{l=k+1}^{(N/2)-1} |y(k)y(l)|^2. \end{aligned} \tag{28}$$

Hence, the absolute value of the correlation function produces the following peak:

$$|P_P(d)| = \sum_{k=0}^{(N/2)-2} \sum_{l=k+1}^{(N/2)-1} |y(k)y(l)|^2 \tag{29}$$

which also shows that $|P_P(d)|$ is not affected by the CFO.

Note that, as aforementioned, a preamble composed of two identical parts in the time domain preserves its periodicity in a frequency-selective fading channel as long as the length of the channel delay spread is smaller than the length of each identical part of the preamble. Hence, the metrics in [3] and [9], and consequently, the proposed metric in (27) are not affected by the frequency-selective channel.

For simplicity in formulation and computational complexity evaluation, we present the proposed metric (27) in a new form. First, the received vector $\mathbf{r}^d = [r(d), r(d+1), \ldots, r(d+N-1)]^T$ is divided into two subvectors, i.e., $\mathbf{r}^d = [r^{d,1}, r^{d,2}]^T$, where

$$r^{d,1} = \{r(d), r(d+1), \ldots, r\left(d+(N/2)-1\right)\} \tag{30}$$

$$\begin{aligned} r^{d,2} = \{&r\left(d+(N/2)\right), r\left(d+(N/2)+1\right) \\ &\ldots, r(d+N-1)\}. \end{aligned} \tag{31}$$

Then, we reorder the elements of $B^{r1,d}$ (21) and $B^{r2,d}$ (22) and write each of them in terms of $(N/2)-1$ subvectors as (32), shown at the bottom of the page, and

$$B^{r2,d} = B^{r1,d+(N/2)} \tag{33}$$

where the nth $(1 \le n \le (N/2)-1)$ subvector of $B^{r1,d}$ is obtained as

$$B_n^{r1,d} = \left[r^{d,1}(0), r^{d,1}(1), \ldots, r^{d,1}\left((N/2)-n-1\right)\right] \circ \left[r^{d,1}(n), r^{d,1}(n+1), \ldots, r^{d,1}\left((N/2)-1\right)\right] \tag{34}$$

where $\circ$ is the Hadamard product (element by element multiplication of the two vectors).

The correlation between the two sequences in (32) and (33), which is equivalent to using the fourth-order elements in (20), is utilized for detection of the presence of the preamble and is expressed as

$$P_P(d) = \sum_{k=0}^{L-1} \overline{B}^{r1,d}(k) B^{r2,d}(k), \quad L \le (N/4)\left((N/2)-1\right) \tag{35}$$

where $\overline{B}^{r1,d}(k)$ denotes the complex conjugate of $B^{r1,d}(k)$, and $L \le (N/4)((N/2)-1)$ is the correlation length that is designed based on the performance expected from the detector. For the proposed timing metric $M_P(d) = 2(|P_P(d)|/R_P(d))$, the normalization function is obtained as

$$R_P(d) = \sum_{k=0}^{L-1} \left|B^{r1,d}(k)\right|^2 + \sum_{k=0}^{L-1} \left|B^{r2,d}(k)\right|^2. \tag{36}$$

The main difference between (23) and (35) is that, in (35), the correlation length $L \le (N/4)((N/2)-1)$ is viewed as a design parameter, according to the expected performance.

V. Analysis and Discussion

Here, we theoretically evaluate the performance of the proposed method. As aforementioned, the frame detection problem is by nature a classification problem, and selection of different classifiers (in this paper timing metrics) is done based on the class separability criterion [15], [18] (the more distinct the classes, the better the timing metrics). To present the performance improvement of the new method, we use two criteria for class separability. The first criterion uses the means of the classifiers (timing metrics) for performance evaluation, and the second criterion is the well-known FDR [15], [18]. Next, we demonstrate that the improvement of the proposed method in separating the classes leads to a significant reduction in the probability of false alarm compared with the previous methods.

A. Performance Evaluation in Terms of Means of Classifiers as a Criterion for Class Separability

As the first criterion for class separability of different timing metrics, we compare their means when the frame is absent and present. The means of the conventional methods [9] in the presence of the preamble (at the correct timing position $d=\theta$) and absence of the preamble (at a wrong timing position $d=\tilde{d}$) are given, respectively, by [9]

$$E\{M_R(\theta)\} \approx \frac{\sigma_y^2}{\sigma_y^2+\sigma_w^2} = \frac{1}{1+(1/\text{SNR})}, \text{(presence of preamble)} \tag{37}$$

$$E\left\{M_R(\tilde{d})\right\} \approx \sqrt{\frac{\pi}{2}\left(\frac{1}{N}\right)}, \text{(absence of preamble)} \tag{38}$$

where $M_R(d) = 2|P_R(d)|/\sum_{k=0}^{N-1}|r(d+k)|^2$, $\sigma_y^2 = E\{|y(k)|^2\}$, and $\text{SNR} = \sigma_y^2/\sigma_w^2$.

The means of the proposed timing metric in the presence and absence of the frame are obtained in Appendixes B and A, respectively, and are as follows:

$$E\{M_P(\theta)\} \approx \frac{\sigma_y^4}{\sigma_y^4+2\sigma_y^2\sigma_w^2+\sigma_w^4} = \frac{1}{1+(2/\text{SNR})+(1/\text{SNR})^2} \quad \text{(presence of preamble)} \tag{39}$$

$$E\left\{M_P(\tilde{d})\right\} \approx \sqrt{\frac{\pi}{2}\left(\frac{1}{2L}\right)}, \text{(absence of preamble)}. \tag{40}$$

$$B^{r1,d} = \left\{B_1^{r1,d}, B_2^{r1,d}, \ldots, B_{(N/2)-1}^{r1,d}\right\} = \left\{\underbrace{r(d)r(d+1), r(d+1)r(d+2), \ldots, r\left(d+(N/2)-2\right)r\left(d+(N/2)-1\right)}_{B_1^{r1,d}}, \right.$$
$$\left. \underbrace{r(d)r(d+2), r(d+1)r(d+3), \ldots, r\left(d+(N/2)-3\right)r\left(d+(N/2)-1\right)}_{B_2^{r1,d}}, \ldots, \underbrace{r(d)r\left(d+(N/2)-1\right)}_{B_{(N/2)-1}^{r1,d}}\right\} \tag{32}$$

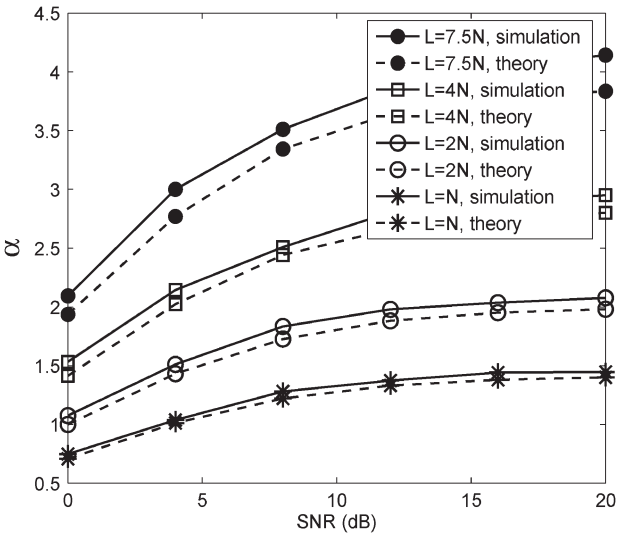

Fig. 2. The factor α (43) for different correlation lengths (L) and SNRs, obtained both theoretically and by simulations in SUI-1 channel ($N = 64$ and $G = 8$).

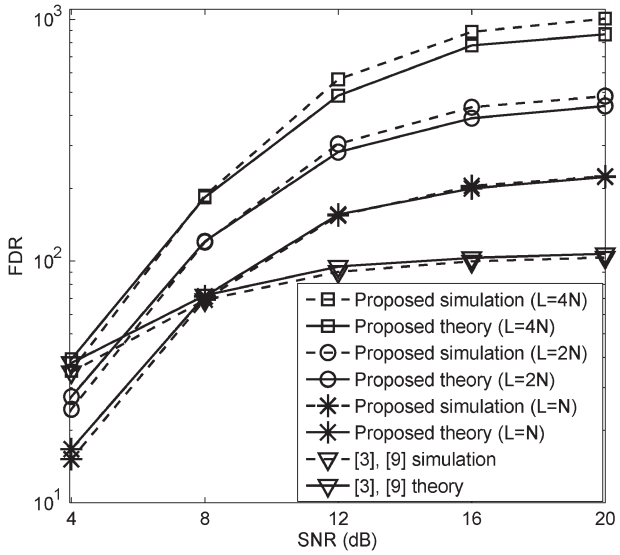

Fig. 3. Fisher's discriminant ratio (FDR) for different timing metrics, obtained both theoretically and by simulations in SUI-1 channel ($N = 64$ and $G = 8$).

Then, we obtain the following factors α_R and α_P for the timing metric proposed in [9] and the new timing metric as

$$\alpha_R = \frac{E\{M_R(\theta)\}}{E\left\{M_R(\tilde{d})\right\}} \approx \frac{1}{(1+(1/\text{SNR}))\sqrt{\frac{\pi}{2}\left(\frac{1}{N}\right)}} \tag{41}$$

$$\alpha_P = \frac{E\{M_P(\theta)\}}{E\left\{M_P(\tilde{d})\right\}} \approx \frac{1}{(1+(2/\text{SNR})+(1/\text{SNR})^2)\sqrt{\frac{\pi}{2}\left(\frac{1}{2L}\right)}}. \tag{42}$$

The timing metric corresponding to the greater factor has a better performance (can better separate the two classes). To demonstrate which of these factors are greater, we define factor α as follows:

$$\alpha = \frac{\alpha_P}{\alpha_R} = \frac{1}{1+(1/\text{SNR})}\sqrt{\frac{2L}{N}}. \tag{43}$$

Note that, in (43), we have shown the pure SNR (not the SNR in decibels). It is obvious that, when $\alpha > 1$, our method achieves better performance in class separability than conventional methods (such as [9]). Considering (43), it is observed that, for SNR > 0 dB, we have $\alpha > 1$ if $L > 2N$. By increasing the SNR, we can also have $\alpha > 1$ for $L < 2N$. For example, for SNR > 4 dB, if $L > N$, we have $\alpha > 1$. In other words, our method can have a better performance even for very low SNRs at the cost of a slight increase in the correlation length. Furthermore, by increasing the SNR and/or the correlation length, a considerably better performance is accomplished.

In Section VII, in Fig. 2, we have illustrated factor α for different SNRs and different values of the correlation length obtained both from analysis and computer simulations. This illustration demonstrates the significant improvement of the new method in separating the classes.

B. Performance Evaluation in Terms of FDR as a Criterion for Class Separability

For a two-class problem, FDR is defined as [18]

$$\text{FDR} = \frac{(\mu_0 - \mu_1)^2}{\sigma_0^2 + \sigma_1^2} \tag{44}$$

where μ_0 and μ_1 are the mean values, and σ_0^2 and σ_1^2 are the variances of the feature (timing metric) in the two classes. FDR, as a widely used measure for class separability, not only applies the means of the feature (timing metric) but also takes advantage of the variances of the feature. Detectors with greater values of FDR can better separate the two classes and consequently have better detection performance.

Now, we calculate FDR for the proposed method and compare it with the conventional methods. For the proposed method using (39), (40), and (64) (see Appendix A), we have $\mu_1 = E\{M_P(\theta)\} \approx (1/(1+(2/\text{SNR})+(1/\text{SNR})^2))$ (in the presence of preamble), $\mu_0 = E\{M_P(\tilde{d})\} \approx \sqrt{(\pi/2)(1/2L)}$ (in the absence of preamble), and $\sigma_0^2 = (2-(\pi/2))(1/2L)$ (in the absence of preamble). The calculation of the variance of the proposed timing metric when the frame is present (σ_1^2) is a laborious task and can involve too many approximations. Hence, we use numerical methods for acquiring the variance of the new timing metric in the presence of the frame. We also calculate FDR for the conventional methods knowing that [9], $\mu_1 = E\{M_R(\theta)\} \approx (1/(1+(1/\text{SNR})))$ (in the presence of preamble), $\mu_0 = E\{M_R(\tilde{d})\} \approx \sqrt{(\pi/2)(1/N)}$ (in the absence of preamble), and $\sigma_0^2 = (2-(\pi/2))(1/N)$ (in the absence of preamble). Furthermore, we have used the numerical methods to obtain the variance of the conventional methods when the frame is present (σ_1^2).

In Section VII, in Fig. 3, we have compared FDR for the proposed scheme with FDR for the previous methods, which shows significant improvement of the new method in terms of class separability.

C. Probability of False Alarm

The probability of false alarm is defined as the probability that, at timing point $\tilde{d}$ that is far away from the correct timing point (none of the samples from $\tilde{d}$ to $\tilde{d}+N-1$ belong to the preamble), the timing metric exceeds predefined threshold λ. Hence, we consider the received vector $\mathbf{r}^d=[r(d),r(d+1),\ldots,r(d+N-1)]^T$ when the preamble is not received, i.e., when we have only noise: $\mathbf{r}^{\tilde{d}}=[w(0),w(1),\ldots,w(N-1)]^T$. The conventional methods [3] and [9] use the following correlation function at a wrong timing point:

$$P(\tilde{d})=\sum_{k=0}^{(N/2)-1}\overline{w}(k)w\left(k+(N/2)\right). \tag{45}$$

In other words, the conventional methods use the noise sample products as $\overline{w}(0)w(N/2)$, $\overline{w}(1)w((N/2)+1),\ldots,\overline{w}((N/2)-1)w(N-1)$, whereas the proposed method is capable of using the following noise products:

$$\begin{aligned}&\{\{\overline{w}(0)\overline{w}(1)w(N/2)w\left((N/2)+1\right),\\&\quad\overline{w}(1)\overline{w}(2)w\left((N/2)+1\right)w\left((N/2)+2\right),\\&\quad\ldots,\overline{w}\left((N/2)-2\right)\overline{w}\left((N/2)-1\right)w(N-2)w(N-1)\},\\&\{\overline{w}(0)\overline{w}(2)w(N/2)w\left((N/2)+2\right),\\&\quad\overline{w}(1)\overline{w}(3)w\left((N/2)+1\right)w\left((N/2)+3\right),\\&\quad\ldots,\overline{w}\left((N/2)-3\right)\overline{w}\left((N/2)-1\right)w(N-3)w(N-1)\},\\&\ldots,\{\overline{w}(0)\overline{w}\left((N/2)-1\right)w(N/2)w(N-1)\}\}.\end{aligned} \tag{46}$$

Since the proposed method can use the correlation between more noise samples and have a longer correlation length than the conventional methods, the new timing metric has a lower probability of false alarm.

To give more insight, we theoretically obtain the probability of false alarm using the statistical properties of the timing metric at an incorrect timing position that is calculated in Appendix A. From Appendix A, we know that, at an incorrect timing position, the timing metric has a Rayleigh distribution with the variance $\sigma_M^2=(2-(\pi/2))(1/2L)$. Hence, the probability of false alarm can be expressed as

$$P\Big(M_P(\tilde{d})>\lambda\Big)=\int_{\lambda}^{\infty}\frac{x}{(1/(2L))}e^{-\frac{x^2}{2\,(1/(2L))}}dx=e^{-L\lambda^2}. \tag{47}$$

In comparison, the probability of false alarm for [9] is given by

$$P\Big(M_R(\tilde{d})>\lambda\Big)=e^{-(N/2)\lambda^2}. \tag{48}$$

Considering (47) and (48), it is observed that the main factor affecting the probability of false alarm is the correlation length (the probability of false alarm decreases as the correlation length increases), which in [9] was limited to $(N/2)$. In other words, our method has a significantly lower probability of false alarm because it can extend the autocorrelation length far beyond the previous methods. Note that L can be chosen up to $(N/4)((N/2)-1)$, i.e., $L\leq(N/4)((N/2)-1)$.

D. Probability of Missed Detection

As aforementioned, the new method uses $B^{r1,d}$ (32) and $B^{r2,d}$ (33) instead of $\mathbf{r}^d$ (that has been used in [3] and [9]) for normalization [see (36)] of the new timing metric. However, at the start of the frame, $B^{r1,d}$ and $B^{r2,d}$ have extra noisy terms in comparison with $\mathbf{r}^d$. As an example, whereas [9] uses $r(d)=s(0)+w(d)$ (here, since the metric is not affected by the CFO, for simplification we have ignored the frequency offset), our scheme utilizes

$$\begin{aligned}r(d)r(d+1)=s(0)s(1)\ &+s(0)w(d+1)\\&+s(1)w(d)+w(d)w(d+1)\end{aligned} \tag{49}$$

which causes the proposed metric to have a smaller peak in comparison with [9]. To make it clear, we mention that, at the correct timing position $d=\theta$, we have the means $E\{M_R(\theta)\}\approx 1/(1+(1/\text{SNR}))$ and $E\{M_P(\theta)\}\approx 1/(1+(2/\text{SNR})+(1/\text{SNR})^2)$ for the conventional methods and proposed method, respectively. Since $(1/\text{SNR})<(2/\text{SNR})+(1/\text{SNR})^2$, it is concluded that $E\{M_R(\theta)\}>E\{M_P(\theta)\}$, which shows that the proposed metric has a smaller peak than [9]. Hence, for high thresholds and low SNRs, it is more likely that the proposed timing metric falls below the threshold and the frame is missed. Thus, the new method has a higher probability of missed detection for high thresholds and low SNRs, where the probability of missed detection is defined as the probability that at the correct timing point, the timing metric falls below a predefined threshold. It is worth mentioning that since the theoretical derivation of the missed detection probability for the new method is an arduous task and can involve too many approximations, we have abstained from its theoretical derivation.

E. Discussion and Combined Method

In Section V-A and B, we indicated the superior performance of the new method in comparison with previous methods in terms of class separability. Here, we give some final remarks about the performance of the new method in terms of the probabilities of false alarm and missed detection obtained in parts C and D.

We investigate the performance first from the SNR point of view and consider three cases: 1) high SNRs; 2) low SNRs and low thresholds; 3) low SNRs and high thresholds. In all three cases, the proposed method has a considerably lower probability of false alarm than the previous schemes [since the probability of false alarm is independent of SNR, as can be observed from (47) and (48)] as will be shown in Section VII. In the first and second cases, the probability of missed detection for the new method is either the same or slightly higher than the previous methods. In the third case, the probability of missed detection for the new method is higher than the previous methods.

From a threshold selection point of view, the three cases of low thresholds, high thresholds and high SNRs, and high thresholds and low SNRs can be considered, In the first and second cases, the probability of missed detection for the new

method and previous methods are the same or nearly the same. In the third case, our method has a higher probability of missed detection.

Taking into account the given remarks and to further improve the detection performance in the third case (either from the SNR or threshold selection points of view), we propose to combine the new method with previous methods (see [3] or [9]) and perform detection based on the threshold values and SNR. When the SNR is high, or when both the SNR and threshold value are low, the proposed timing metric is applied. When the SNR is low and the threshold value is high, methods such as that in [9] are utilized. This combination of the new detector and the previous detectors significantly extends the range of thresholds with an acceptable performance, which results in easier threshold selection (as will be shown in Section VII). In Section VII, we show the improvement caused by the combined method and explain how our method can be used in combination with previous methods for different values of threshold and SNR.

It is worth mentioning that, as demonstrated in (28), the fourth-order statistics generated from the two identical parts of the received preamble remain identical, except for a phase shift of $2\pi v$. Hence, $|P_P(d)|$ and, consequently, the timing metric $M_P(d)$ are not affected by the CFO [as shown in (29)].

VI. Computational Complexity and Frame Synchronization

Here, we first evaluate the computational complexity of the proposed method and then address frame synchronization utilizing the new method.

A. Computational Complexity

To evaluate the computational complexity, we consider the correlation function of the new method $P_P(d)$ [see (35)]. Without loss of generality, we assume that $B^{r1,d}$ and $B^{r2,d}$ consist of only their first subvectors. At the timing instants d and $d+1$, we, respectively, have

$$\begin{aligned} B^{r1,d} &= \left\{B_1^{r1,d}\right\} \\ &= [r(d)r(d+1), r(d+1)r(d+2), \\ &\quad \ldots, r\left(d+(N/2)-2\right) r\left(d+(N/2)-1\right)] \quad (50) \\ B^{r1,d+1} &= \left\{B_1^{r1,d+1}\right\} \\ &= [r(d+1)r(d+2), r(d+2)r(d+3), \\ &\quad \ldots, r\left(d+(N/2)-1\right) r\left(d+(N/2)\right)]. \quad (51) \end{aligned}$$

Considering (50) and (51), the elements of $B^{r1,d+1}$ can be written in terms of the elements of $B^{r1,d}$ as

$$\begin{aligned} B^{r1,d+1} = \big[&B^{r1,d}(1), B^{r1,d}(2), \ldots, B^{r1,d}\left((N/2)-2\right), \\ &r\left(d+(N/2)-1\right) r\left(d+(N/2)\right)\big]. \quad (52) \end{aligned}$$

TABLE I
Computational Complexity of Frame Detectors

Method	Multiplications	Additions
Schmidl [3]	2	2
Ruan [9]	2	2
Proposed	$6N_s$, $1 \le N_s \le (N/2)-1$	$2N_s$, $1 \le N_s \le (N/2)-1$

In the same way, $B^{r2,d+1}$ is obtained as

$$\begin{aligned} B^{r2,d+1} = \big[&B^{r2,d}(1), B^{r2,d}(2), \ldots, B^{r2,d}\left((N/2)-2\right), \\ &r(d+N-1)r(d+N)\big]. \quad (53) \end{aligned}$$

Finally, $P_P(d)$ in (35) can be written in the recursive form as

$$\begin{aligned} P_P(d+1) &= P_P(d) - \overline{B}^{r1,d}(0)B^{r2,d}(0) \\ &\quad + \overline{B}^{r1,d+1}\left((N/2)-2\right) B^{r2,d+1}\left((N/2)-2\right). \quad (54) \end{aligned}$$

Hence, for each subvector of $B^{r1,d}$ and $B^{r2,d}$, we need six complex multiplications and two complex additions to compute $P_P(d)$ at each timing instant d.

It is worth mentioning that the correlation function of the conventional methods $P_R(d) = \sum_{k=0}^{(N/2)-1} \overline{r}(d+k)r(d+k+(N/2))$ can be obtained in the following recursive form [3]:

$$\begin{aligned} P_R(d+1) &= P_R(d) - \overline{r}(d)r\left(d+(N/2)\right) \\ &\quad + \overline{r}\left(d+(N/2)\right) r(d+N). \quad (55) \end{aligned}$$

Hence, for the correlation function of the conventional methods, two complex multiplications and two complex additions are needed at each timing instant d.

In Table I, we have demonstrated the computational complexity of different frame detectors, where N_s is the number of subvectors of $B^{r1,d}$ and $B^{r2,d}$ that is used in the correlation function. It is observed that our method has higher complexity. Note that the number of subvectors N_s, $1 \le N_s \le (N/2)-1$, is designed based on the correlation length, the performance expected from the detector, and the affordable system complexity.

B. Frame Synchronization

To describe how the new frame detection method can improve the overall frame synchronization procedure, we consider the two stages of frame synchronization: 1) detecting the preamble and 2) finding the start of the frame in the following N samples. The frame is detected when a timing metric reaches a predefined threshold, and the start of the frame is usually determined based on the maximum value of a timing metric. Once the frame is detected, finding the start of the frame within the following N samples can happen independently of the frame detection stage. It means that our proposed timing metric, which is mainly designed for the detection purpose, can be coupled with any timing metrics that estimate the start of the frame, such as the timing metrics in [3] and [9], and improve the overall synchronization performance. This improvement in the synchronization performance is caused by the fact that

the performance of the timing estimator (of the start of the frame) is greatly dependent and affected by the frame detector performance.

We will demonstrate in Section VII the significant performance improvement in the frame synchronization resulting from the utilization of the new frame detection.

Furthermore, since the complexity of the correlation functions was obtained and shown in Table I at each timing instant d (independent of whether they are used for frame detection or estimation of the start of the frame), the complexity of the two synchronization stages is independently assessed. For example, assume that, at the timing instant $d = d'$, the frame is detected. At each timing instant $d \leq d'$, the complexity of the frame detector is considered as the required computational complexity, and for each timing instant after $d = d'$, the complexity of the estimator of the start of the frame is considered as the required computational complexity. Hence, in either of the two stages, depending on what timing metric is utilized, the computational complexity can be found in Table I.

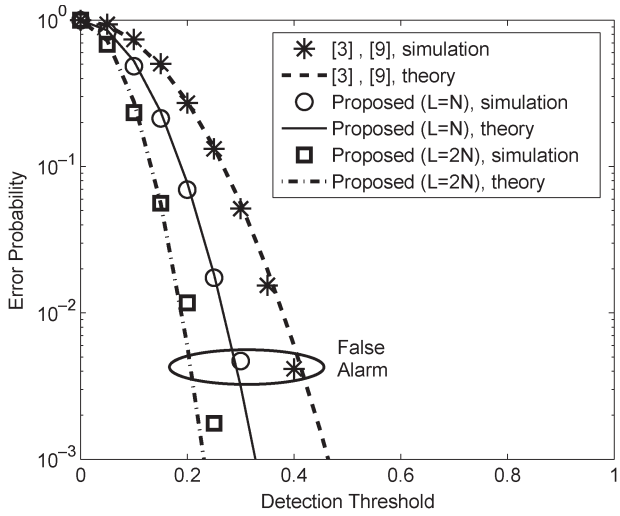

Fig. 4. Probability of false alarm obtained both from theoretical analysis and simulation ($N = 64$ and $G = 8$).

VII. Results

Computer simulations have been used to assess the performance of the new method. We have considered an OFDM system with $N = 64$ subcarriers, the CP length of $G = 8$, and the sampling rate of 5.5 MHz. Stanford University Interim (SUI) channel modeling (SUI-1) [23] has been utilized to simulate a frequency-selective fading channel. Furthermore, the normalized CFO is set to $v = 12.5$ (note that the actual frequency offset $\triangle f$ is in the range $0 \leq \triangle f < f_s$, where f_s is the sampling frequency, which makes the normalized frequency offset by the subcarrier spacing $v = \triangle f/(f_s/N) = N\triangle f/f_s$ be in the range $0 \leq v < N$ or equivalently $-(N/2) \leq v < (N/2)$ [3]).

In Fig. 2, we have depicted factor $\alpha = \alpha_P/\alpha_R = 1/(1 + (1/\text{SNR}))\sqrt{(2L/N)}$ [see (43)] for different values of SNR and correlation length obtained both from analysis and computer simulations. When $\alpha > 1$, we have $\alpha_P > \alpha_R$, and our method improves performance. According to this figure, the new method achieves better performance in separating the classes and consequently makes the difference between the values of the new timing metric at the correct and wrong timing points greater than the difference between the values of the conventional timing metric at the correct and wrong timing points.

According to this figure, for all correlation lengths depicted, our method has a better performance ($\alpha > 1$) for SNR > 4 dB. Moreover, for $L \geq 2N$, the new method improves the performance for SNR > 0 dB.

Fig. 3 compares FDR for the new metric with the conventional metrics for different values of SNR and correlation length. It is obvious that the proposed method has a significantly higher FDR and, consequently, better class separability performance. For example, for a correlation length of $L = 4N$, our method outperforms the conventional methods for SNR $>$ 4 dB, or for a correlation length of $L = 2N$, our method has a considerably better performance for SNR > 6 dB, compared with previous methods.

In Fig. 4, we have depicted the false alarm probability obtained both from the theoretical analysis and simulation. It is evident that the proposed method has a considerably lower probability of false alarm due to having an extended autocorrelation length. It is noticed that the performance of the new method improves as the correlation length increases. We also observe that the simulation results verify the analytical evaluations.

Note that, in Figs. 2–4, there are some discrepancies between the theoretical and simulation results. This difference mainly results from the approximation of the pdf of the correlation function of the proposed timing metric with a Gaussian pdf using the central limit theorem (CLT) for dependent random variables (as obtained in Appendix A). As the length of the correlation increases, the dependence between the samples increases, and the accuracy of the pdf approximation decreases, which explains why the difference between the theoretical and simulation results increases with the correlation length.

In Figs. 5 and 6, we have depicted the probability of false alarm along with the probability of missed detection for different detectors at SNR $= 15$ dB and SNR $= 12$ dB, respectively. We have illustrated the performance of the new method, for different values of the correlation length L. From the figures, it is obvious that the proposed method has a significantly better performance in terms of the probability of false alarm. Further, as the correlation length increases, the performance improves. It is also observed that the new method has a slightly higher probability of missed detection.

To show the overall performance of the new frame detector when utilized in coarse timing estimation and since the goal of coarse timing estimation is to obtain an ISI-free region of OFDM symbols, we have obtained the probability of timing estimation errors that cause ISI. In these simulations, the performance of the new method is attained when the proposed detector is followed by the following metric (proposed in [9]) for estimation of the start of the frame:

$$M_R(d) = \frac{2\left|\sum_{k=0}^{(N/2)-1} \overline{r}(d+k)r\left(d+k+(N/2)\right)\right|}{\sum_{k=0}^{N-1}|r(d+k)|^2}. \quad (56)$$

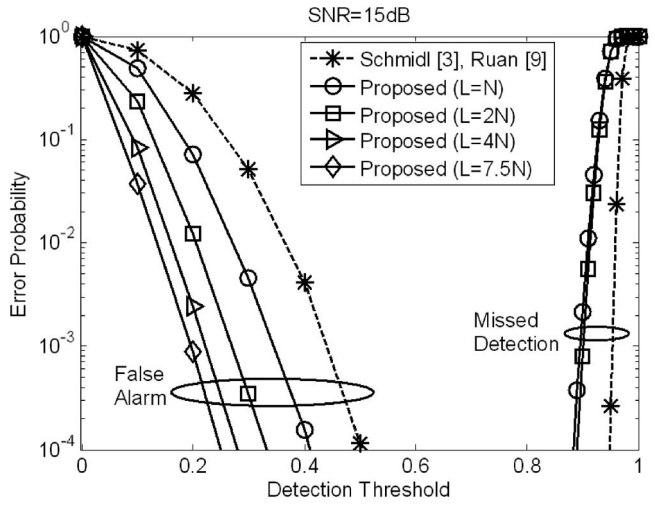

Fig. 5. Probability of false alarm and missed detection for different detectors in SUI-1 channel at SNR = 15 dB ($N = 64$ and $G = 8$).

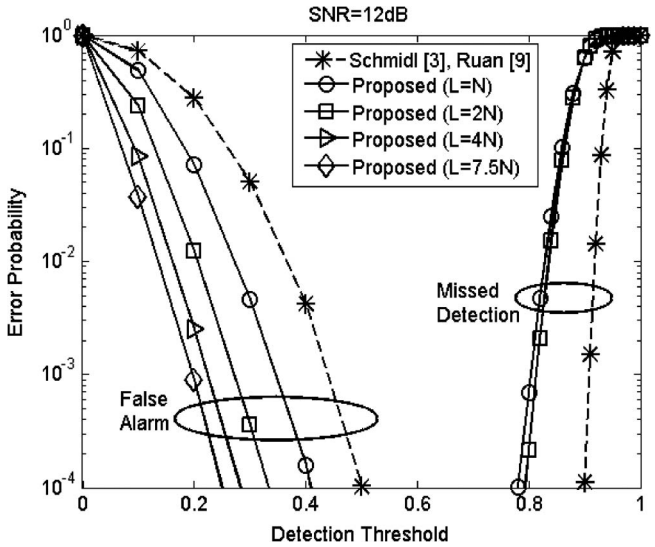

Fig. 6. Probability of false alarm and missed detection for different detectors in SUI-1 channel at SNR = 12 dB ($N = 64$ and $G = 8$).

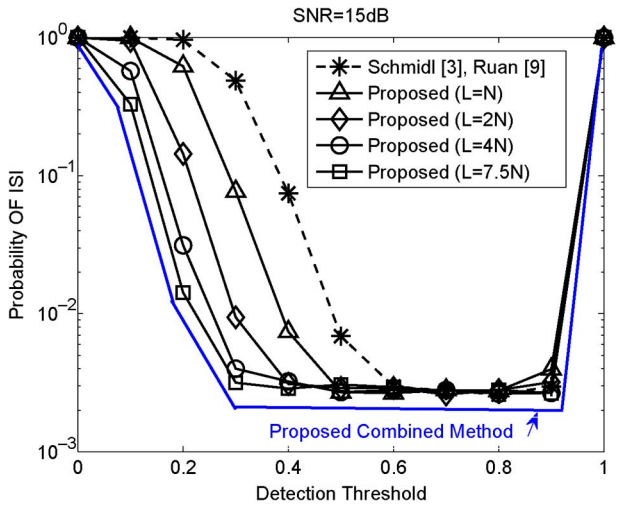

Fig. 7. Probability of timing errors that cause ISI in SUI-1 channel at SNR = 15 dB ($N = 64$ and $G = 8$).

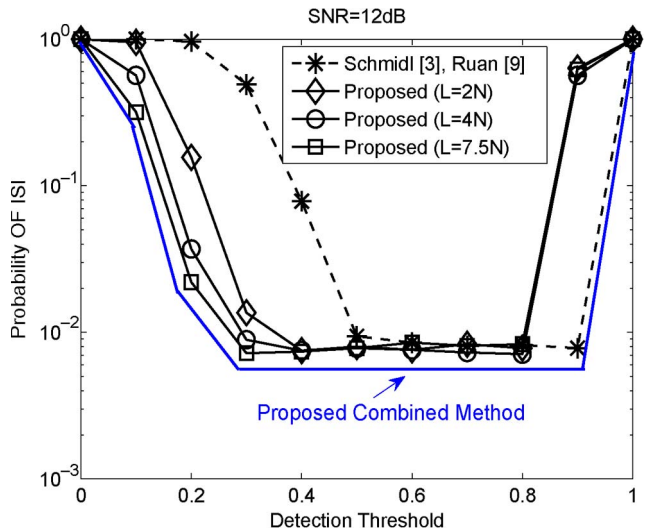

Fig. 8. Probability of timing errors that cause ISI in SUI-1 channel at SNR = 12 dB ($N = 64$ and $G = 8$).

Fig. 7 shows the probability of ISI for different estimators at SNR = 15 dB. It is obvious that the new method has a lower probability of ISI for a wider range of threshold values. The new method has a probability of ISI below 10^{-2} for threshold values $0.3 \leq \eta \leq 0.9$, whereas in [3] and [9], this probability of ISI occurs for threshold values $0.5 \leq \eta \leq 0.9$. According to this figure, when the SNR is high enough, the combination of the new method with the previous methods (as mentioned in Section V and indicated in the figure as "proposed combined method") does not increase the range of acceptable threshold values (since previous methods does not have a better performance for any thresholds than the new method).

In Fig. 8, at SNR = 12 dB, it is noticed that the probability of ISI for the proposed method falls below 10^{-2} for $0.3 \leq \eta \leq 0.8$ and falls below 10^{-2} for $0.5 \leq \eta \leq 0.9$ for the conventional methods. Hence, our method provides a wider range of acceptable threshold values. However, by comparing Fig. 7 with Fig. 8, it is observed that the decrease in the SNR has reduced the range of suitable thresholds. In this case, if the new method is combined with the previous schemes, as shown in the figure, the range of acceptable thresholds is increased up to $0.3 \leq \eta \leq 0.9$.

Fig. 9 demonstrates the probability of ISI at SNR = 9 dB. In this figure, the probability of ISI for the proposed method falls below 10^{-1} for $0.2 \leq \eta \leq 0.7$ and falls below 10^{-1} for $0.5 \leq \eta \leq 0.8$ for the conventional methods, which shows that not only does the new scheme have a considerably wider range of thresholds with satisfactory performance, but in addition, its combination with the previous method provides a wider range of suitable thresholds $(0.2 \leq \eta \leq 0.8)$.

In Fig. 10, for having a probability of ISI below 10^{-1} at SNR = 6 dB, the threshold value should be chosen in the range $0.2 \leq \eta \leq 0.5$ for the new method and should be in the range $0.5 \leq \eta \leq 0.7$ for the conventional methods. Furthermore, when our method is used in combination with previous methods, the range of thresholds with the lowest probability of ISI considerably increases. As a result, for having a probability

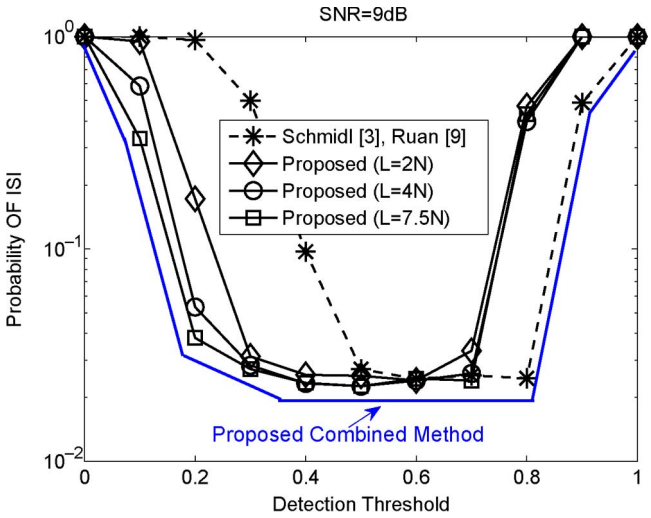

Fig. 9. Probability of timing errors that cause ISI in SUI-1 channel at SNR $=$ 9 dB ($N = 64$ and $G = 8$).

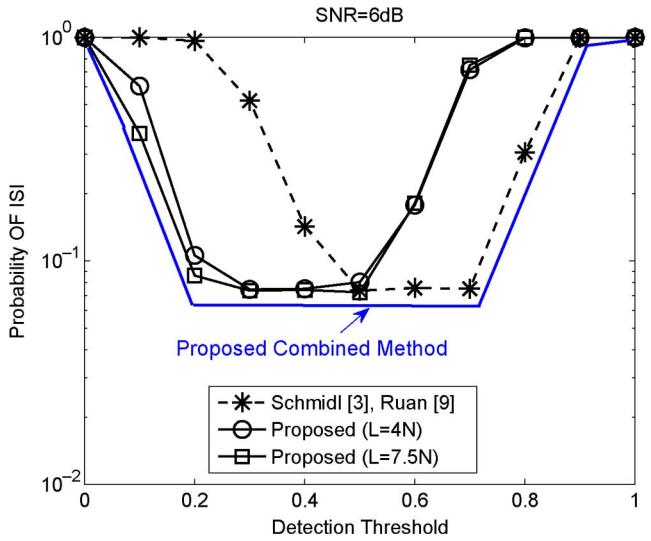

Fig. 10. Probability of timing errors that cause ISI in SUI-1 channel at SNR $=$ 6 dB ($N = 64$ and $G = 8$).

of ISI below 10^{-1}, the threshold can have any values in the range $0.2 \leq \eta \leq 0.7$.

To give more insight into how our detection method can be combined with previous methods, we consider Figs. 7–10. In these figures, it is observed that, for a range of thresholds, the new method and conventional schemes have the same performance (probability of ISI). For example, in Fig. 9, at SNR $=$ 9 dB, for threshold values $0.5 \leq \eta \leq 0.7$, the new method and conventional schemes have nearly the same probability of ISI. These thresholds (for which the new method and previous ones have the same performance) can be chosen as the changing points for the methods to be used. For instance, in Fig. 9, at SNR $= 9$ dB, for $0 \leq \eta \leq 0.6$, our method can be used and for $0.6 < \eta \leq 1$, the conventional methods can be utilized. It is also observed in Figs. 7–10 that the range of thresholds for which the new methods and previous methods have the same performance is mainly affected by the SNR, and with the decreases in the SNR, this range becomes smaller. However, for the SNRs considered in practical situations (SNR ≥ 7 dB), there exists thresholds for which our method and previous methods have the same performance.

Looking again in Fig. 7, when the SNR is relatively high (SNR $= 15$ dB), there is no need for any combination with previous methods. In addition, in Figs. 7–10, for low thresholds $0 \leq \eta \leq 0.5$, our method has better performance than previous methods. Therefore, it is concluded from these figures that, when the SNR is relatively high or for low thresholds, there is no need for any combinations. However, when the SNR is relatively low and for high thresholds (e.g., SNR $= 9$ dB and $\eta > 0.7$ in Fig. 9, or SNR $= 6$ dB and $\eta > 0.5$ in Fig. 10) the combination with previous methods can improve the performance.

It is concluded that the new method not only significantly increases the range of suitable threshold values by itself but also its combination with previous schemes can provide a considerably wider range of threshold values with acceptable performance and make choosing an appropriate threshold remarkably easier.

VIII. Conclusion

In this paper, we have investigated the problem of frame detection in OFDM systems. We demonstrated that sufficient statistics for detection of a preamble composed of two identical parts in the time domain do not exist, and conventional methods are not optimal. A new scheme for frame detection was developed using the fourth-order statistics, and its improved performance was indicated in terms of different class separability criteria and probability of false alarm. The computational complexity of the proposed scheme was obtained. It was shown that the new method can significantly improve the detection performance and its application in coarse timing estimation can significantly extend the range of acceptable threshold values.

Appendix A
Statistical Properties of the Proposed Timing Metric at Wrong Timing Points

To derive the distribution of the timing metric at a wrong timing point, first, we consider an M-dependent sequence. A stationary random sequence $\{Y_i\}_{i=1}^{\infty}$ is called M-dependent if there is a nonnegative integer M such that the sequences $\{Y_i\}_{i=1}^{\delta}$ and $\{Y_i\}_{i=\varepsilon}^{\infty}$ are statistically independent for all $\varepsilon \geq \delta \geq 1$ satisfying $\varepsilon - \delta > M$ [24]. We have the following CLT for an M-dependent sequence [24]:

Theorem 1: Suppose that $\{Y_i\}_{i=1}^{\infty}$ is a stationary M-dependent sequence and that

$$E\{Y_1\} = 0 \text{ and } E\left\{Y_1^2\right\} < \infty. \tag{57}$$

Define

$$\sigma^2 = E\left\{Y_1^2\right\} + 2\sum_{j=1}^{m} E\left\{Y_1 Y_{j+1}\right\}. \tag{58}$$

Then, if $\sigma^2 > 0$, the sum

$$\sum_{i=1}^{n} Y_i/\sqrt{n} \tag{59}$$

is asymptotically normally distributed with zero mean and variance σ^2.

Now, we consider the received vector at timing point $\tilde{d}$ that is far away from the correct timing point (none of the samples from $\tilde{d}$ to $\tilde{d}+N-1$ belong to the preamble), i.e., when the received vector contains only noise samples $\mathbf{r}^{\tilde{d}} = [w(0), w(1), \ldots, w(N-1)]^T$. In this condition and for moderate values of the correlation length L, it is easy to show that the sequence produced by element-by-element multiplication of $\overline{B}^{r1,\tilde{d}}$ and $B^{r2,\tilde{d}}$ is an M-dependent sequence. In other words, the elements of $B^{\tilde{d}}$ given by

$$B^{\tilde{d}} = \overline{B}^{r1,\tilde{d}} \circ B^{r2,\tilde{d}} \tag{60}$$

is an M-dependent sequence, where $\circ$ denotes the Hadamard product (the element-by-element multiplication of the two vectors). Hence, according to the CLT for an M-dependent sequence (*Theorem 1*), at an incorrect timing position

$$P_P(\tilde{d}) = \sum_{k=0}^{L-1} \overline{B}^{r1,\tilde{d}}(k) B^{r2,\tilde{d}}(k) = \sum_{k=0}^{L-1} B^{\tilde{d}}(k) \tag{61}$$

or

$$P_P(\tilde{d}) = \sum_{k=0}^{L-1} \mathrm{Re}\left\{B^{\tilde{d}}(k)\right\} + \sum_{k=0}^{L-1} \mathrm{Im}\left\{B^{\tilde{d}}(k)\right\} \tag{62}$$

as the summation of a large number of uncorrelated elements of an M-dependent sequence [see (61)] can be approximated as the summation of two Gaussian distributions with zero mean and variance $L\sigma_w^8/2$ [see (62)] (note that, each of $\mathrm{Re}\{B^{\tilde{d}}(k)\}$ and $\mathrm{Im}\{B^{\tilde{d}}(k)\}$ has a Gaussian distribution with zero mean and variance $\sigma_w^8/2$), where $\mathrm{Re}\{B^{\tilde{d}}(k)\}$ and $\mathrm{Im}\{B^{\tilde{d}}(k)\}$ denote the real and imaginary parts of $B^{\tilde{d}}(k)$, respectively, and σ_w^8 is the variance of $B^{\tilde{d}}(k)$. Hence, $|P_P(\tilde{d})|$ has a Rayleigh distribution with the variance $\mathrm{Var}\{|P_P(\tilde{d})|\} = (2-(\pi/2))(L\sigma_w^8/2)$.

Next, similar to [9], by substituting $R_P(\tilde{d})$ with its mean $E\{R_P(\tilde{d})\} = 2L\sigma_w^4$, it is concluded that the timing metric

$$M_P(\tilde{d}) \approx 2\frac{\left|P_P(\tilde{d})\right|}{E\left\{R_P(\tilde{d})\right\}} = \frac{\left|P_P(\tilde{d})\right|}{L\sigma_w^4} \tag{63}$$

has approximately a Rayleigh distribution with the following variance:

$$\sigma_M^2 = \mathrm{Var}\left\{M_P(\tilde{d})\right\} = \left(2-\frac{\pi}{2}\right)\frac{L\sigma_w^8}{2L^2\sigma_w^8} = \left(2-\frac{\pi}{2}\right)\frac{1}{2L}. \tag{64}$$

Appendix B
Mean of the Proposed Timing Metric at the Correct Timing Position

To obtain the mean of the correlation and normalization functions, without loss of generality, we consider the case in which $B^{r1,d}$ and $B^{r2,d}$ have only their first subvectors, i.e., $B^{r1,d} = \{B_1^{r1,d}\}$, $B^{r2,d} = \{B_1^{r2,d}\}$, and $L = (N/2) - 1$.

At the correct timing point $(d = \theta)$, we have $r(k) = e^{j(2\pi/N)kv} y(k-\theta) + w(k)$, $0 \le k \le N-1$, and $y(k) = y(k+(N/2))$, $0 \le k \le N-1$. Hence, $P_P(d)$ can be written as

$$\begin{aligned} P_P(d) = &\sum_{k=0}^{(N/2)-2} \overline{r}(d+k)\overline{r}(d+k+1) r\left(d+k+(N/2)\right) \\ &\times r\left(d+k+(N/2)+1\right) \\ P_P(\theta) = &\sum_{k=0}^{(N/2)-2} \left(e^{-j\frac{2\pi}{N}kv}\overline{y}(k) + \overline{w}(k)\right) \\ &\times \left(e^{-j\frac{2\pi}{N}(k+1)v}\overline{y}(k+1) + \overline{w}(k+1)\right) \\ &\times \left(e^{j\frac{2\pi}{N}(k+(N/2))v} y(k) + w\left(k+(N/2)\right)\right) \\ &\cdot \left(e^{j\frac{2\pi}{N}(k+(N/2)+1)v} y(k+1) + w\left(k+(N/2)+1\right)\right) \end{aligned} \tag{65}$$

or equivalently

$$\begin{aligned} P_P(\theta) = &\sum_{k=0}^{(N/2)-2} \left(e^{-j\frac{2\pi}{N}(2k+1)v}\overline{y}(k)\overline{y}(k+1) + \overline{w'}(k)\right) \\ &\left(e^{j\frac{2\pi}{N}(2k+1+N)v} y(k)y(k+1) + w''(k)\right) \end{aligned} \tag{66}$$

where

$$\begin{aligned} w'(k) = &e^{j\frac{2\pi}{N}(k+1)v} y(k+1)w(k) \\ &+ e^{j\frac{2\pi}{N}kv} y(k)w(k+1) + w(k)w(k+1) \end{aligned} \tag{67}$$

$$\begin{aligned} w''(k) = &e^{j\frac{2\pi}{N}(k+(N/2)+1)v} y(k+1) w\left(k+(N/2)\right) \\ &+ e^{j\frac{2\pi}{N}(k+(N/2))v} y(k) w\left(k+1+(N/2)\right) \\ &+ w\left(k+(N/2)\right) w\left(k+(N/2)+1\right). \end{aligned} \tag{68}$$

Furthermore, $P_P(\theta)$ can be expressed as

$$P_P(\theta) = e^{j2\pi v} \sum_{k=0}^{(N/2)-2} |y(k)|^2 |y(k+1)|^2 + w'''(k) \tag{69}$$

where

$$\begin{aligned} w'''(k) = &e^{j\frac{2\pi}{N}(2k+1+N)v} y(k)y(k+1)\overline{w'}(k) \\ &+ e^{-j\frac{2\pi}{N}(2k+1)v}\overline{y}(k)\overline{y}(k+1)w''(k) + \overline{w'}(k)w''(k). \end{aligned} \tag{70}$$

Finally, the mean of $|P_P(d)|$ at the correct timing point ($d=\theta$) is expressed as

$$E\{|P_P(\theta)|\} \approx \sum_{k=0}^{(N/2)-2} E\left\{|y(k)|^2 |y(k+1)|^2\right\} = ((N/2)-1)\sigma_y^4 = L\sigma_y^4 \quad (71)$$

where L is the correlation length, and $\sigma_y^2 = E\{|y(k)|^2\}$ is the signal power after passing through a multipath fading channel.

On the other hand, at the correct timing point, the normalization function can be written as

$$R_P(d) = \sum_{k=0}^{(N/2)-2} |r(d+k)r(d+k+1)|^2 + \sum_{k=0}^{(N/2)-2} |r(d+k+(N/2))\, r(d+k+(N/2)+1)|^2 \quad (72)$$

$$R_P(\theta) = \sum_{k=0}^{(N/2)-2} \left|e^{j\frac{2\pi}{N}(2k+1)v} y(k)y(k+1) + w'(k)\right|^2 + \sum_{k=0}^{(N/2)-2} \left|e^{j\frac{2\pi}{N}(2k+1+N)v} y(k)y(k+1) + w''(k)\right|^2. \quad (73)$$

Therefore, knowing that $E\{|w'(k)|^2\} = 2\sigma_y^2\sigma_w^2 + \sigma_w^4$, we have

$$\begin{aligned} E\{R_P(\theta)\} &= 2E\left\{\sum_{k=0}^{(N/2)-2} \left|e^{j\frac{2\pi}{N}(2k+1)v} y(k)y(k+1) + w'(k)\right|^2\right\} \\ &= 2\sum_{k=0}^{(N/2)-2} E\left\{|y(k)y(k+1)|^2 + |w'(k)|^2\right\} \\ &= 2((N/2)-1)\left(\sigma_y^4 + 2\sigma_y^2\sigma_w^2 + \sigma_w^4\right) \\ &= 2L\left(\sigma_y^4 + 2\sigma_y^2\sigma_w^2 + \sigma_w^4\right). \end{aligned} \quad (74)$$

Following the same reasoning, it can be concluded that for any correlation length L

$$E\{|P_P(\theta)|\} = L\sigma_y^4 \quad (75)$$

$$E\{R_P(\theta)\} = 2L\left(\sigma_y^4 + 2\sigma_y^2\sigma_w^2 + \sigma_w^4\right). \quad (76)$$

Finally, the mean of the proposed timing metric can be approximated as

$$E\{M_P(\theta)\} \approx 2\frac{E\{|P_P(\theta)|\}}{E\{R_P(\theta)\}} = \frac{\sigma_y^4}{\sigma_y^4 + 2\sigma_y^2\sigma_w^2 + \sigma_w^4} = \frac{1}{1 + (2/\mathrm{SNR}) + (1/\mathrm{SNR})^2}. \quad (77)$$

REFERENCES

[1] W. L. Chin, "Blind symbol synchronization for OFDM systems using cyclic prefix in time-variant and long- echo fading channels," *IEEE Trans. Veh. Technol.*, vol. 61, no. 1, pp. 185–195, Jan. 2012.

[2] W. L. Chin, "ML estimation of timing and frequency offsets using distinctive correlation characteristics of OFDM signals over dispersive fading channels," *IEEE Trans. Veh. Technol.*, vol. 60, no. 2, pp. 444–456, Feb. 2011.

[3] T. M. Schmidl and D. C. Cox, "Robust frequency and timing synchronization for OFDM," *IEEE Trans. Commun.*, vol. 45, no. 12, pp. 1613–1621, Dec. 1997.

[4] H. Minn, M. Zeng, and V. K. Bhargava, "On timing offset estimation for OFDM systems," *IEEE Commun. Lett.*, vol. 4, no. 7, pp. 242–244, Jul. 2000.

[5] H. Minn, V. K. Bhargava, and K. B. Letaief, "A robust timing and frequency synchronization for OFDM systems," *IEEE Trans. Wireless Commun.*, vol. 2, no. 4, pp. 822–839, Jul. 2003.

[6] A. J. Coulson, "Maximum likelihood synchronization for OFDM using a pilot symbol: Algorithm," *IEEE J. Sel. Areas Commun.*, vol. 19, no. 12, pp. 2486–2494, Dec. 2001.

[7] A. J. Coulson, "Maximum likelihood synchronization for OFDM using a pilot symbol: Analysis," *IEEE J. Sel. Areas Commun.*, vol. 19, no. 12, pp. 2495–2503, Dec. 2001.

[8] K. Shi and E. Serpedin, "Coarse frame and carrier synchronization of OFDM systems: A new metric and comparison," *IEEE Trans. Wireless Commun.*, vol. 3, no. 4, pp. 1271–1284, Jul. 2004.

[9] M. Ruan, M. C. Reed, and Z. Shi, "Training symbol based coarse timing synchronization in OFDM systems," *IEEE Trans. Wireless Commun.*, vol. 8, no. 5, pp. 2558–2569, May 2009.

[10] H. Abdzadeh-Ziabari and M. G. Shayesteh, "Robust timing and frequency synchronization for OFDM systems," *IEEE Trans. Veh. Technol.*, vol. 60, no. 8, pp. 3646–3656, Oct. 2011.

[11] G. Ren, Y. Chang, H. Zhang, and H. Zhang, "Synchronization methods based on a new constant envelope preamble for OFDM systems," *IEEE Trans. Broadcast.*, vol. 51, no. 1, pp. 139–143, Mar. 2005.

[12] Y. Kang, S. Kim, D. Ahn, and H. Lee, "Timing estimation for OFDM systems by using a correlation sequence of preamble," *IEEE Trans. Consum. Electron.*, vol. 54, no. 4, pp. 1600–1608, Nov. 2008.

[13] J. Choi, J. Lee, Q. Zhao, and H. Lou, "Joint ML estimation of frame timing and carrier frequency offset for OFDM systems employing time-domain repeated preamble," *IEEE Trans. Wireless Commun.*, vol. 9, no. 1, pp. 311–317, Jan. 2010.

[14] H. Hsieh and W. Wu, "Maximum likelihood timing and carrier frequency offset estimation for OFDM systems with periodic preambles," *IEEE Trans. Veh. Technol.*, vol. 58, no. 8, pp. 4224–4237, Oct. 2009.

[15] Y. Zhang, A. B. Baggeroer, and J. G. Bellingham, "The total variance of a periodogram-based spectral estimate of a stochastic process with spectral uncertainty and its application to classifier design," *IEEE Trans. Signal Process.*, vol. 53, no. 12, pp. 4556–4567, Dec. 2005.

[16] G. B. Giannakis and M. K. Tsatsanis, "Signal detection and classification using matched filtering and higher order statistics," *IEEE Trans. Acoust., Speech, Signal Process.*, vol. 38, no. 7, pp. 1284–1296, Jul. 1990.

[17] B. M. Sadler, G. B. Giannakis, and K.-S. Lii, "Estimation and detection in non-Gaussian noise using higher order statistics," *IEEE Trans. Signal Process.*, vol. 42, no. 10, pp. 2729–2741, Oct. 1994.

[18] S. Theodoridis and K. Koutroumbas, *Pattern Recognition, Fourth Edition,* 4th ed. San Francisco, CA, USA: Academic, 2008.

[19] *(Amendment and Corrigendum to IEEE Std. 802.16–2004): IEEE Standard for Local and Metropolitan Area Networks Part 16: Air Interface for Fixed and Mobile Broadband Wireless Access Systems Amendment2: Physical and Medium Access Control Layers for Combined Fixed and Mobile Operation in Licensed Bands and Corrigendum 1*, IEEE Std. 802.16e–2005/IEEE Std. 802.16-2004/Cor 1–2005, 2006.

[20] S. Chaudhari, V. Koivunen, and H. V. Poor, "Autocorrelation-based decentralized sequential detection of OFDM signals in cognitive radios," *IEEE Trans. Signal Process.*, vol. 57, no. 7, pp. 2690–2700, Jul. 2009.

[21] M. A. Richards, *Fundamentals of Radar Signal Processing*. NewYork, NY, USA: McGraw-Hill, 2005.

[22] S. M. Kay, *Fundamentals of Statistical Signal Processing: Detection Theory*. Englewood Cliffs, NJ, USA: Prentice-Hall, 1998.

[23] V. Erceg, K. V. S. Hari, M. S. Smith, and D. S. Baum, "Channel models for fixed wireless applications," ETH Zürich, Zurich, Switzerland, Tech. Rep. IEEE 802.16a-03/01, Jul. 2003.

[24] H. V. Poor and J. B. Thomas, "Memoryless discrete-time detection of a constant signal in M-dependent noise," *IEEE Trans. Inf. Theory*, vol. IT-25, no. 1, pp. 54–61, Jan. 1979.

Hamed Abdzadeh-Ziabari received the B.S. degree in electrical engineering from the Islamic Azad University of Karaj, Karaj, Iran, and the M.S. degree in electrical engineering from Urmia University, Urmia, Iran.

He is currently with the Department of Electrical Engineering, Urmia University. His research interests include signal processing techniques for wireless communication systems, with emphasis on synchronization algorithms in orthogonal frequency-division multiplexing and orthogonal frequency-division multiple-access systems.

Mahrokh G. Shayesteh (M'04) received the B.S. degree from the University of Tehran, Tehran, Iran; the M.S. degree from Khajeh Nassir University of Technology, Tehran; and the Ph.D. degree from Amir Kabir University of Technology, Tehran, all in electrical engineering.

She is currently an Associate Professor with Urmia University, Urmia, Iran. She is also working with the Wireless Research Laboratory, Advanced Communications Research Institute, Department of Electrical Engineering, Sharif University of Technology, Tehran. Her research interests include wireless communication systems, spread spectrum, and image processing.